A High-Q Time-Variant Bandpass Filter

Bahman Abolhassani and Mohammad Khalaj-Amirhosseini

***Abstract*—A high-Q time-variant (TV) band-pass filter (BPF) is analyzed in this paper. *N* parallel identical low-pass RC filters make this BPF, in which each of these *N* filters is sequentially switched on for an equal time interval, periodically. The resulting BPF provides a stable frequency response and is insensitive to element variations. Through mathematical analysis, equations are derived for the frequency response and the bandwidth of the BPF. Moreover, the validity of these equations is confirmed by experimental results. These equations make the design of the above high-Q BPF an easy task.**

***Index Terms*—*N*-path Filters, switched capacitor filters, high-Q bandpass filters, time-variant filters.**

I. Introduction

High-Q band-pass filters (BPFs) are required in many applications such as tracking signals, SNR (signal to noise power ratio) enhancement in frequency modulation (FM), and in rejection of power-line signals [1]-[4]. Realization of high-Q BPFs, especially for audio signals, is quite difficult. High-Q BPFs may be realized by active RC filters. However, the frequency response of such filters is quite sensitive to element-value variations. Moreover, such filters can be unstable for high-Q values.

Switched capacitor filters (SCFs) are another class of filters, which provides a practical method for a fully integrated realization of high quality filters. Exact methods are available for designing SCFs [1]. Typical sensitivities of SCFs are lower than 0.1 dB/1% element-value change [2]. However, high-Q SCFs are still sensitive to element value variations, which can also make them unstable.

N-path filters are introduced to reduce the sensitivity of high-Q band pass SCFs [3]. *N*-path filters are linear time-variant (LTV), which make the analysis of the filter a difficult task [3]. These filters have N identical switched capacitor filters that each of them is periodically (with a period of NT_S) placed between the input and output terminals for a time duration of T_S. Fig. 1 shows a simplified *N*-path SCF, which employs a first order low pass filter for each path. This paper presents a mathematical analysis for the *N*-path filter shown in Fig. 1. The novelty of this work is derivation of closed form mathematical equations for both the frequency response and the bandwidth of the time-variant N-path filter. This makes the design procedure of a high-Q BPF as easy as designing known analog filters. The analysis is confirmed by experimental results. The design procedure of such filters is also explained briefly.

Manuscript received February 23, 2005; revised July 21, 2005.

The authors are with the Electrical Engineering Department, Iran University of Science and Technology, Narmak, Tehran 16845, I. R. Iran (email: abolhassani@iust.ac.ir, khalaja@iust.ac.ir).

Publisher Item Identifier S 1682-0053(06)0343

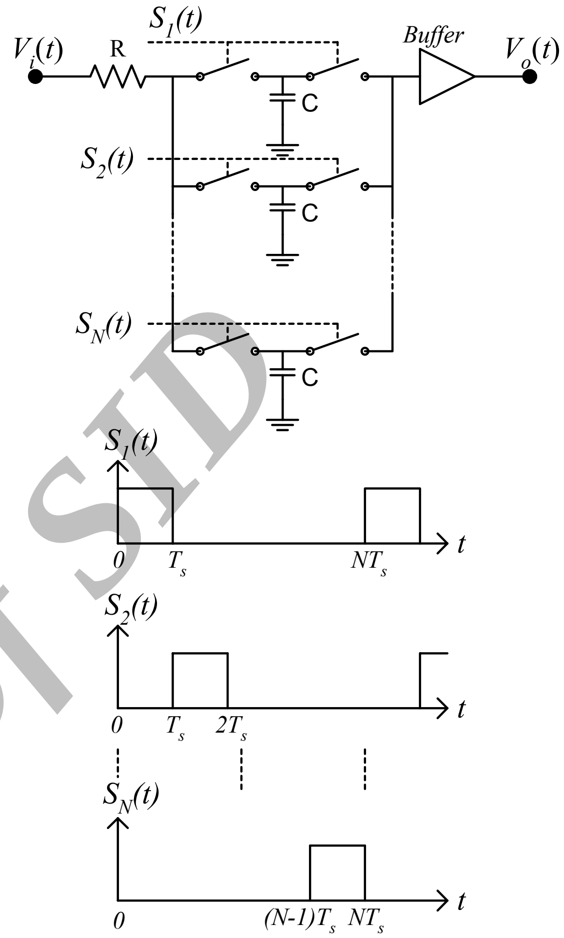

Fig. 1. A Simplified circuit of an *N*-path filter.

The remainder of this paper is organized as follows. Sections II and III present the mathematical analysis of the *N*-path filter. Closed form mathematical equations are derived for the frequency response and bandwidth of the filter. In Section IV, the mathematical analysis is verified by experimental results. Section V presents conclusions of this work.

II. Analysis of the Filter

In this section, closed form equations are derived for the frequency response and the bandwidth of the N-path filter. Each of N paths is considered to have the same time-constant $\tau_0 = RC$. The analysis is done by applying a single frequency signal $v_i(t) = \exp(j\omega_0 t)$ as the filter input. The output signal of the filter $v_O(t)$ is given by

$$v_o(t) = \int_{-\infty}^{\infty} v_i(\tau) h_\tau(t) d\tau \qquad (1)$$

where $v_i(\tau)$ is the input signal at time τ and $h_\tau(t)$ is the filter impulse response at time t to an impulse applied at time τ.

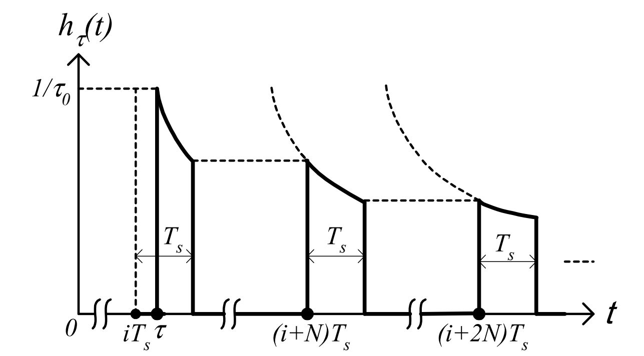

Fig. 2. *N*-path filter impulse response.

Since the N-path filter is linear time variant [3], the filter impulse response depends on both τ and t.

The filter impulse response $h_\tau(t)$, i.e., the response to input $\delta(t-\tau)$, is shown in Fig. 2, where $iT_S < \tau < (i+1)T_S$. At $t = \tau$, only one of N capacitors (say the capacitor of the first path) is connected between the input and output terminals. The input impulse charges the above capacitor to a maximum voltage of $1/\tau_0$ volts since the output voltage is $1/\tau_0 \exp\left(-(t-\tau)/\tau_0\right)$ for $iT_S < t < (i+1)T_S$. The capacitor starts discharging for $\tau < t < (i+1)T_S$. After this time, the capacitor is opened and hence the output voltage remains constant until time $t = (i+N)T_S$. For $(i+N)T_S < t < (i+N+1)T_S$, the capacitor restarts discharging. The process of voltage discharging for the duration of T_s and zero output voltage for the duration of $(N-1)T_S$ repeats as long as the capacitor has any voltage. So, for $iT_S < \tau < (i+1)T_S$ the impulse response is given by

$$h_\tau(t) = \frac{1}{\tau_0}\exp(-(t-\tau)/\tau_0)\left[u(t-\tau) - u\left(t-(i+1)T_S\right)\right] + \frac{1}{\tau_0}\sum_{n=1}^{\infty}\left\{\exp\left(-\left(t-\tau-n(N-1)T_S\right)/\tau_0\right)\left[u\left(t-(i+nN)T_S\right) - u\left(t-(i+nN+1)T_S\right)\right]\right\} \quad (2)$$

In (1), replacing $v_i(t)$ by $\exp(j\omega_0 t)$, and $h_\tau(t)$ by (2), the output voltage of the filter becomes

$$v_o(t) = \sum_{i=-\infty}^{\infty}\int_{iT_S}^{(i+1)T_S}\exp(j\omega_0\tau)h_\tau(t)\,d\tau \quad (3)$$

Appendix A presents detailed calculation of $v_o(t)$ whose final result is given by

$$v_o(t) = \sum_{i=-\infty}^{\infty}\left\{\frac{\exp(j\omega_0 t)}{1+j\omega_0\tau_0}\times\left[1-\exp\left(-(j\omega_0+1/\tau_0)(t-iT_s)\right)\right]\prod\left(\frac{t-(i+0.5)T_s}{T_s}\right) - \frac{\exp\left((j\omega_0+1/\tau_0)iT_s\right)}{1+j\omega_0\tau_0}\left[1-\exp\left((j\omega_0+1/\tau_0)T_s\right)\right]\times\sum_{n=1}^{\infty}\exp\left(-\frac{t-n(N-1)T_s}{\tau_0}\right)\prod\left(\frac{t-(i+nN+0.5)T_s}{T_s}\right)\right\} \quad (4)$$

where $\prod(t/T_S) = 1$ for $|t| \le T_S/2$ and is equal to zero for other times.

Fourier transform of $v_o(t)$, is given by

$$V_o(j\omega) = \left\{-\frac{2\sinh\left((j\omega+1/\tau_0)T_s/2\right)}{T_s\tau_0(j\omega_0+1/\tau_0)(j\omega+1/\tau_0)}\times\frac{1-\exp\left(-j(N\omega-\omega_0)T_s\right)}{1-\exp\left(-(jN\omega+1/\tau_0)T_s\right)}\exp\left(-(j\omega+1/\tau_0)T_s/2\right) + \frac{\exp\left(-j(\omega-\omega_0)T_s/2\right)}{\tau_0(j\omega_0+1/\tau_0)}\operatorname{sinc}\left((f-f_0)T_s\right)\right\}\times\sum_{i=-\infty}^{\infty}\delta\left(f-(f_0+if_s)\right) \quad (5)$$

where $\operatorname{sinc}(x) = \sin(\pi x)/(\pi x)$, $f = \omega/(2\pi)$, $f_0 = \omega_0/(2\pi)$ and $f_S = 1/T_S$.

As it is seen in (5), for the single-tone input signal, i.e., $v_i(t) = \exp(j\omega_0 t)$ corresponding with $V_i(f) = \delta(f-f_0)$, there are infinite number of tones at the output of the filter. Similar results can be obtained for the input signal $v_i(t) = \exp(-j\omega_0 t)$. So, for the input signal $v_i(t) = \cos(\omega_0 t)$, the output tones are located around $\pm f_0$ and are separated by if_S, where $i = 0, \pm 1, \pm 2, \ldots$. If f_S is chosen to be very larger than $2f_0$, then undesired frequency components, i.e., $\delta\left(f \pm f_0 + if_s\right)$ for $i \ne 0$, can be eliminated by cascading the *N*-path filter with a simple lowpass filter whose bandwidth is smaller than $f_S - f_0$. In this case, the resulted filter behaves like a linear time invariant (LTI) circuit.

Considering undesired frequency components are eliminated, as explained above, the frequency response of the resulted LTI filter (that is $H(j\omega) = V_O(j\omega)/V_i(j\omega)$, where $V_i(j\omega) = \delta(f-f_0)$) is obtained from the RHS of (5) by removing the terms under the Σ for $i \ne 0$. By replacing $1/\tau_0$ by ω_c and T_S by $2\pi/\omega_s$, $H(j\omega)$ simplifies to

$$H(j\omega) = -\frac{\omega_c}{j\omega+\omega_c}\left\{\frac{\sinh\left((j\omega+1/\tau_0)\pi/\omega_s\right)}{(j\omega+\omega_c)\pi/\omega_s}\times\frac{1-\exp\left(-j2\pi(N-1)\omega/\omega_s\right)}{1-\exp\left(-2\pi(jN\omega+\omega_c)/\omega_s\right)}\exp\left(-\pi(j\omega+\omega_c)/\omega_s\right) - 1\right\} \quad (6)$$

If the amplitude and phase of $H(j\omega)$ are plotted, it is observed that at frequencies $f_r = mf_S/N$, where $m = 0, 1, 2, \ldots$, the amplitude has local maximums and the value of the phase is zero. The amplitude of the absolute maximum is unit, which is at $\omega = 0$. By increasing ω, the amplitude of local maximums reduces. To eliminate local maximums at frequencies $f_r = mf_S/N$ for $m \ge 2$, one can cascade another simple filter with the *N*-path filter.

III. The Bandwidth of the Filter

In this section, the bandwidth of the filter is derived at frequencies corresponding to the local maximums. Practical values for $\tau_0 = 1/\omega_c$, ω_s and ω_0 dictate that the relation $\omega_c \ll \omega = \omega_0 \ll \omega_S$ must hold. So, $|H(j\omega)|$ is approximated as

$$|H(j\omega)| \cong \frac{\omega_c}{\omega}|\operatorname{sinc}(\omega/\omega_s)\times\frac{1-\exp\left(-j2\pi(N-1)\omega/\omega_s\right)}{\left(1-\exp(-2\pi\omega_c/\omega_s)\exp(-j2\pi N\omega/\omega_s)\right)}\exp(-j\pi\omega/\omega_s) - 1| \quad (7)$$

Around the frequencies $\omega = \omega_r = m\omega_S/N$, at which the amplitude of frequency response has local maximums, the denominator in (7) tends to zero and hence the term -1 in (7) can be neglected. Therefore, it can be written as

$$
\begin{aligned}
&|H(j\omega \cong jm\omega_s/N)| \\
&\cong \frac{(\omega_c/\omega)\left|\operatorname{sinc}(\omega/\omega_s)\left[1-\exp\left(-j2\pi(N-1)\omega/\omega_s\right)\right]\right|}{\sqrt{\left(1-\exp(-2\pi\omega_c/\omega_s)\right)^2+4\exp(-2\pi\omega_c/\omega_s)\sin^2(\pi N\omega/\omega_s)}}, \\
&\cong \frac{(\omega_c/\omega)\left|\operatorname{sinc}(\omega/\omega_s)\left[1-\exp\left(-j2\pi(N-1)\omega/\omega_s\right)\right]\right|}{\left(1-\exp(-2\pi\omega_c/\omega_s)\right)\sqrt{1+\dfrac{\sin^2(\pi N\omega/\omega_s)}{\sinh^2(\pi\omega_c/\omega_s)}}}, \\
&= \frac{(\omega_c/\omega)\left|2\operatorname{sinc}(\omega/\omega_s)\sin\left(\pi(N-1)\omega/\omega_s\right)\right|}{\left(1-\exp(-2\pi\omega_c/\omega_s)\right)\sqrt{1+\dfrac{\sin^2(\pi N\omega/\omega_s)}{\sinh^2(\pi\omega_c/\omega_s)}}}, \qquad (8) \\
&\cong \frac{(\omega_c/\omega)\left|2\operatorname{sinc}(\omega/\omega_s)\sin\left(\pi\omega/\omega_s\right)\right|}{\left(1-\exp(-2\pi\omega_c/\omega_s)\right)\sqrt{1+\dfrac{\sin^2(\pi N\omega/\omega_s)}{\sinh^2(\pi\omega_c/\omega_s)}}}, \\
&= \frac{2\pi\omega_c/\omega_s}{1-\exp(-2\pi\omega_c/\omega_s)}\frac{\operatorname{sinc}^2(\omega/\omega_s)}{\sqrt{1+\dfrac{\sin^2(\pi N\omega/\omega_s)}{\sinh^2(\pi\omega_c/\omega_s)}}}
\end{aligned}
$$

To find out the filter bandwidth around $\omega=\omega_r=m\omega_S/N$, ω is replaced by $\omega+\Delta\omega$ in (8), and the amplitude is equated to $1/\sqrt{2}$ times of that of $\omega_r=m\omega_S/N$. In this case,

$$
\begin{aligned}
&\left|H\left(j(m\omega_s/N+\Delta\omega)\right)\right| = \frac{1}{\sqrt{2}}\left|H(jm\omega_s/N)\right| \\
&= \frac{1}{\sqrt{2}}\times 2\pi\frac{\omega_c}{\omega_s}\frac{\operatorname{sinc}^2(m/N)}{1-\exp(-2\pi\omega_c/\omega_s)} \qquad (9)
\end{aligned}
$$

Assuming $\Delta\omega$ is much smaller than $\omega_r = m\omega_S/N$, the following approximation can be written.

$$\operatorname{sinc}^2(m/N+\Delta\omega/\omega_s) \cong \operatorname{sinc}^2(m/N) \qquad (10)$$

Using (7), and (10), (9) is given by

$$
\begin{aligned}
&\left|\sin\left(\pi N(m\omega_s/N+\Delta\omega)/\omega_s\right)\right| = \sin\left(\pi N\Delta\omega/\omega_s\right) \\
&= \sinh(\pi\omega_c/\omega_s) \qquad (11)
\end{aligned}
$$

Hence, the half of the filter bandwidth is obtained as

$$\Delta\omega \cong \frac{\omega_c}{N} = \frac{1}{N\tau_0} \qquad (12)$$

Replacing τ_0 by RC of each path in the *N*-path filter, the bandwidth BW is given by

$$BW = \frac{2\Delta\omega}{2\pi} \cong \frac{1}{\pi NRC} \qquad (13)$$

As it is seen in (13), the filter bandwidth is dependent on the value of *N*, as well as to the time constant $\tau_0 = RC$. The bandwidth can be adjusted simply by adjusting the values of N, R, and C. It is notable that the bandwidth is not dependent on the center frequency f_r. As was mentioned before, f_s and N are chosen such that $f_r = f_S/N$. So for a given N, adjusting the bandwidth does not affect the center frequency and vice versa.

For tracking a signal whose frequency is f, we have to design the filter such that f_S/N be equal to f_0. Moreover, as mentioned before, f_S should be chosen to have a large value. So for small f, N must be chosen to be large as well. It is also notable that N times of f is applied as the clock for the filter so that variation in f results in variation of the clock, and therefore, the filter tracks the frequency of the input signal.

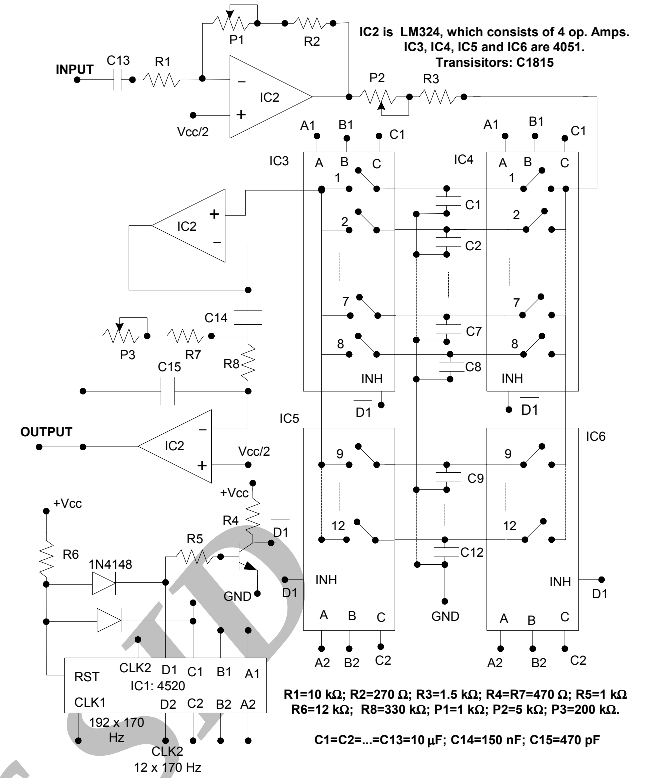

Fig. 3. The Circuit of an implemented high-Q bandpass filter.

IV. Experimental Results

For verification of the analysis, an *N*-path filter was implemented whose center frequency and bandwidth are $f_r = 170$ Hz and $\mathrm{BW} = 0.9$ Hz, respectively. The quality factor of this filter is $Q = f_r/BW = 188.8$, which is much larger than practical values for Q of conventional time-invariant filters. The circuit of this high-Q BPF is shown in Fig. 3.

The values for N and f_S were chosen to be 12 and 12×170 Hz, respectively. This makes undesired output frequencies quite far from center frequency such that they can be eliminated easily by a simple BPF whose center frequency is f_r and its higher edge is smaller than $f_s - f_r$. Each of capacitors C1 to C12 has a capacity of 10 μF. Due to having tolerances in the element values, R was chosen to be a series of two resistors: R3 (a constant resistor) and P2 (a variable resistor). This facilitates adjusting the bandwidth of the filter to 0.9 Hz at which R=P2+R3 was 2950 Ω according to (13). To eliminate undesired frequency components (11×170, 13×170, … Hz) and undesired local maximums (2×170, 3×170, … Hz), a simple BPF with a center frequency of about 170 Hz and a bandwidth of smaller than 100 Hz was employed. This filter is placed right before the output terminal in Fig. 3. As well, a buffer is placed between this BPF and the *N*-path filter to eliminate their loading effects on each other.

To measure the output amplitude at different frequencies, a high resolution signal generator and a frequency divider was used as the input to the circuit. The frequency step of the input signal was 0.1 Hz.

The magnitude of the frequency response $|H(jf)|$ obtained from the measurement, as well as from (6) is shown in Fig. 4, over a small frequency span around $f_r = 170$ Hz so that the experimental and theoretical values

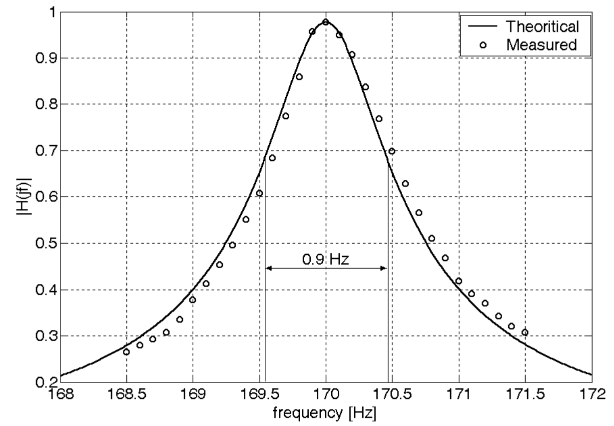

Fig. 4. The amplitude of the frequency response of the implemented filter.

can be compared easily. As shown, the theoretical and measured values are quite close, which results in the validity of our analysis. Moreover, the measured value for the bandwidth was 0.9 Hz, which equals the theoretical value obtained from (13). This confirms the validity of (13).

V. Conclusions

A high-Q N-path filter was analyzed and mathematical equations were derived for the frequency response and bandwidth of the filter. These equations can be used to design high-Q bandpass filters using N-path filters. The validity of these equations was confirmed by experimental results. The design procedure for a high-Q bandpass tracking filter was also described.

Appendix A

The output voltage, $v_0(t)$, given by (4) is calculated here. Starting from (3), first $\int_{iT_S}^{(i+1)T_S}\exp(j\omega_0\tau)h_\tau(t)d\tau$ is broken into three integrals: I_1, I_2, and I_3, and each of them is calculated below

$$I_1 = \frac{1}{\tau_0}\int_{iT_S}^{(i+1)T_S}\exp(j\omega_0\tau)\exp\left(-(t-\tau)/\tau_0\right)u(t-\tau)d\tau \quad \text{(A.1)}$$

By changing the variable t-τ to z, I_1 can be calculated for three cases of $t < iT_S$, $iT_S < t < (i+1)T_S$ and $t > (i+1)T_S$. By doing so, I_1 is given by

$$\begin{aligned} I_1 = \frac{\exp(j\omega_0 t)}{1+j\omega_0\tau_0}&\Big\{\left[1-\exp\left(-(j\omega_0+1/\tau_0)(t-iT_s)\right)\right] \\ &\times\left[u(t-iT_s)-u\left(t-(i+1)T_S\right)\right] \\ &-\left[1-\exp\left((j\omega_0+1/\tau_0)T_s\right)\right] \\ &\times\exp\left(-(j\omega_0+1/\tau_0)(t-iT_s)\right)u\left(t-(i+1)T_S\right)\Big\} \end{aligned} \quad \text{(A.2)}$$

Now, I_2 is calculated

$$\begin{aligned} I_2 &= \frac{-1}{\tau_0}\int_{iT_S}^{(i+1)T_S}\exp(j\omega_0\tau)\exp\left(-(t-\tau)/\tau_0\right)u\left(t-(i+1)T_s\right)d\tau \\ &= \frac{\exp(-t/\tau_0)}{1+j\omega_0\tau_0}\left[1-\exp\left((j\omega_0+1/\tau_0)T_s\right)\right] \\ &\quad\times\exp\left((j\omega_0+1/\tau_0)iT_s\right)u\left(t-(i+1)T_S\right) \end{aligned} \quad \text{(A.3)}$$

Calculation of I_3 is given below

$$\begin{aligned} I_3 &= \frac{1}{\tau_0}\sum_{n=1}^{\infty}\Bigg\{\int_{iT_S}^{(i+1)T_S}\exp(j\omega_0\tau)\exp\Big(-\frac{t-\tau-n(N-1)T_s}{\tau_0}\Big)d\tau \\ &\quad\times\left[u\left(t-(i+nN)T_s\right)-u\left(t-(i+nN+1)T_S\right)\right]\Bigg\} \\ &= -\frac{\exp\left((j\omega_0+1/\tau_0)T_s\right)}{1+j\omega_0\tau_0}\left[1-\exp\left((j\omega_0+1/\tau_0)T_s\right)\right] \\ &\quad\times\left[u\left(t-(i+nN)T_s\right)-u\left(t-(i+nN+1)T_s\right)\right] \\ &\quad\times\sum_{n=1}^{\infty}\exp\left(-\frac{t-n(N-1)T_s}{\tau_0}\right) \end{aligned} \quad \text{(A.4)}$$

Summation of I_1, I_2 and I_3 is the final result, which is given in (4).

Appendix B

Fourier transform of $v_o(t)$, given by (5), is calculated in this section. First, the Fourier transform of $\exp(-at)\prod\left((t-t_0)/T_s\right)$ is calculated that is

$$\begin{aligned} &\int_{t_0-T_s/2}^{t_0+T_s/2}\exp(-at)\exp(-j\omega t)dt \\ &= \frac{2}{a+j\omega}\exp\left(-(a+j\omega)t_0\right)\sinh\left((a+j\omega)T_s/2\right) \end{aligned} \quad \text{(B.1)}$$

Using the above Fourier transform, then $V_O(j\omega)$ is obtained from (4) as follows

$$\begin{aligned} V_o(j\omega) &= -\frac{2\sinh\left((j\omega+1/\tau_0)T_s/2\right)}{\tau_0(j\omega_0+1/\tau_0)(j\omega+1/\tau_0)}\left[1-\exp\left((j\omega+1/\tau_0)T_s\right)\right] \\ &\quad\times\sum_{i=-\infty}^{\infty}\sum_{n=1}^{\infty}\Big[\exp\left(n(N-1)T_s/\tau_0\right)\exp\left((j\omega_0+1/\tau_0)iT_s\right) \\ &\qquad\exp\left(-(j\omega+1/\tau_0)(i+nN+0.5)T_s\right)\Big] \\ &\quad+\frac{2\sin\left((\omega-\omega_0)T_s/2\right)}{\tau_0(j\omega_0+1/\tau_0)(\omega-\omega_0)}\sum_{n=1}^{\infty}\exp\left(-j(\omega-\omega_0)(i+0.5)T_s\right) \\ &\quad-\frac{2\sinh\left((j\omega+1/\tau_0)T_s/2\right)}{\tau_0(j\omega_0+1/\tau_0)(j\omega+1/\tau_0)} \\ &\quad\times\sum_{i=-\infty}^{\infty}\exp\left((j\omega_0+1/\tau_0)iT_s\right)\exp\left(-(j\omega+1/\tau_0)(i+0.5)T_s\right) \end{aligned} \quad \text{(B.2)}$$

Knowing

$$\sum_{n=1}^{\infty}\exp\left(-n(jN\omega+1/\tau_0)T_s\right) = \frac{\exp\left(-(jN\omega+1/\tau_0)T_s\right)}{1-\exp\left(-(jN\omega+1/\tau_0)T_s\right)} \quad \text{(B.3)}$$

and the Poisson equation, which is

$$\sum_{i=-\infty}^{\infty}\exp(-j\omega iT_s) = \frac{1}{T_s}\sum_{i=-\infty}^{\infty}\delta(f-\frac{i}{T_s}) \quad \text{(B.4)}$$

$V_O(j\omega)$ can be simplified as given in (5).

References

[1] P. A. Allen, *Switched Capacitor Circuits*, Van Nostrand Reinhold, 1984.

[2] M. B. Ghaderi, J. Nossek, and G. Temes, "Narrow-band switched capacitor bandpass filters," *IEEE Trans. on Circuits and Systems*, vol. 29, no. 8, pp. 557-571, Aug. 1982.

[3] L. E. Franks and I. W. Sandberg, "An alternative approach to the realization of network functions: The N-path filter," *Bell System Technical Journal*, pp. 1321-1350, Sep. 1960.

[4] L. Chen, *A Phase Domain Adaptive Tracking Bandpass Filter for Power Engineering Applications*, MA.Sc. Thesis, University of Toronto, Canada, 1994.

Bahman Abolhassani was born in Tehran, Iran. He received the B.Sc. degree from Iran University of Science and Technology (IUST), Tehran, Iran and the M.Sc. and Ph.D. degrees from the University of Saskatchewan, Saskatoon, Sk, Canada, all in electrical engineering.

He worked at the College of Water and Power Technology, Tehran, Iran, as an Instrumentation Engineer for three years. Then, he worked in a number of private and government companies, as a Communication Engineer. He joined the Department of Electrical Engineering, IUST as a Lecturer in communication systems. He also served as a Sessional Lecturer at the University of Saskatchewan. Currently, he is an Assistant Professor and Head of the Electrical Engineering Department at IUST. His research interests are in the field of wireless communications, especially indoor wireless communications, network planning, spread spectrum and code division multiple access techniques. He is a member of the Institute of Electrical and Electronics Engineers (IEEE).

Mohammad Khalaj-Amirhosseini was born in Tehran, Iran, in 1969. He received his B.Sc., M.Sc., and Ph.D. degrees from Iran University of Science and Technology (IUST) in 1992, 1994, and 1998 respectively, all in Electrical Engineering. He is currently an Associate Professor at the College of Electrical Engineering of IUST. His scientific fields of interest are electromagnetic direct and inverse problems including microwaves, antennas and high frequency circuits.